Microvascular inflammation in the absence of HLA-DSA and C4d: an orphan category in Banff classification with cytotoxic T and NK cell infiltration

Anna Buxeda, MD[1,2]*, Laura Llinàs-Mallol, PhD[1,2]*, Javier Gimeno, MD[2,3], Dolores Redondo-Pachón, MD, PhD[1,2], Carlos Arias-Cabrales, MD, PhD[1,2], Carla Burballa, MD, PhD[1,2], Adrián Puche, MD[3], Miguel López-Botet, MD, PhD[2,4], José Yélamos, PhD[2,5], Carlos Vilches, MD, PhD[6], Maarten Naesens, MD, PhD[7], María José Pérez-Sáez, MD, PhD[1,2], Julio Pascual, MD, PhD[2,8,†] and Marta Crespo, MD, PhD[1,2,†,#].

[1] Department of Nephrology, Hospital del Mar, Barcelona, Spain.

[2] Hospital del Mar Medical Research Institute (IMIM), Barcelona, Spain.

[3] Department of Pathology, Hospital del Mar, Barcelona, Spain.

[4] Universitat Pompeu Fabra, Barcelona, Spain

[5] Department of Immunology, Hospital del Mar, Barcelona, Spain

[6] Immunogenetics-HLA, Instituto de Investigación Sanitaria Puerta de Hierro Segovia de Arana, Majadahonda, Madrid, Spain.

[7]Department of Microbiology, Immunology and Transplantation, KU Leuven, Leuven, Belgium.

[8] Department of Nephrology, Hospital Universitario 12 de Octubre, Madrid, Spain.

* *These authors contributed equally*

[†] *Senior authors*

ORCID:

Anna Buxeda, http://orcid.org/0000-0001-7305-3259;

Laura Llinàs-Mallol, http://orcid.org/0000-0003-4696-3331;

Miguel López-Botet, http://orcid.org/0000-0003-4882-065X;

José Yélamos, http://orcid.org/0000-0003-1195-1496;

Carlos Vilches, http://orcid.org/0000-0002-0300-9225;

María José Pérez-Sáez, http://orcid.org/0000-0002-8601-2699;

Julio Pascual, http://orcid.org/0000-0002-4735-7838;

Marta Crespo, http://orcid.org/0000-0001-6992-6379;

[#]**Corresponding author:**

Marta Crespo, MD, PhD.

Nephrology Department. Hospital del Mar.

Passeig Marítim, 25-29. 08003 Barcelona, Spain.

Tel: +34 932483162.

Email: mcrespo@psmar.cat

Running title: Immunological characterization of microvascular inflammation histology.

ABBREVIATIONS:

ABMR: Antibody-mediated rejection; DSA: Donor-specific antibodies; eGFR: Estimated glomerular filtration rate; EM: Electron microscope; FFPE: Formalin-fixed paraffin-embedded; g: Glomerulitis; HLA: Human leukocyte antigens; IFTA: Interstitial fibrosis and tubular atrophy; Ig: Immunoglobulin; IQR: Interquartile range; KT: Kidney transplantation; MPA: Mycophenolic acid; mTORi: Mammalian target of rapamycin inhibitors; MVI: Microvascular inflammation; iMVI: isolated microvascular inflammation; NK: Natural killer cell; PBL: Peripheral blood lymphocytes; ptc: Peritubular capillaritis; sABMR: Suspicious for antibody-mediated rejection; SD: Standard deviation; TCMR: T-cell mediated rejection.

ABSTRACT

Isolated microvascular inflammation (iMVI) without HLA donor-specific antibodies or C4d deposition in peritubular capillaries remains an enigmatic phenotype, which cannot be categorized as antibody-mediated rejection (ABMR) in recent Banff classifications. We included 221 kidney transplant recipients with biopsies with ABMR (n=73), iMVI (n=32), and normal (n=116) diagnoses. We compared peripheral blood leukocyte distribution by flow cytometry and inflammatory infiltrates in kidney transplant biopsies among groups. Flow cytometry showed less lymphocytes and total, $CD4^+$, and $CD8^+$ peripheral T cells in iMVI compared with ABMR and normal cases. ABMR and iMVI had fewer total Natural Killer (NK) cells but more $NKG2A^+$ NK cells. Immunohistochemistry indicated that ABMR and iMVI had higher $CD3^+$ and $CD68^+$ glomerular infiltration than normal biopsies, whereas $CD8^+$ and $TIA1^+$ cells only increased in iMVI, suggesting they are cytotoxic T cells. Peritubular capillaries displayed more $CD3^+$, $CD56^+$, $TIA1^+$, and $CD68^+$ cells in both ABMR and iMVI. In contrast, iMVI had less plasma cell infiltration in peritubular capillaries and interstitial aggregates than ABMR. iMVI displayed decreased circulating T and NK cells mirrored by a T cell and NK cell infiltration in the renal allograft, similar to ABMR. However, a lesser plasma cell infiltration in iMVI may suggest an antibody-independent underlying stimulus.

Abstract word count: 201 words.
Significance statements word count: 124 words.
Manuscript word count: Total: (3910+abst) = 4111 words.

Keywords: Antibody-mediated rejection, immune cell, immunohistochemistry, kidney biopsy, kidney transplantation, microvascular inflammation

SIGNIFICANCE STATEMENTS

What is already known about this subject: Isolated microvascular inflammation (iMVI), defined as MVI histology without HLA-DSA or C4d deposition, cannot be classified as ABMR according to Banff classification despite being a negative prognostic indicator of graft survival.

What this study adds: the present study identifies significant inflammatory infiltrate alterations in iMVI biopsies, showing intense cytotoxic T cell and NK cell infiltration, similar to ABMR. However, the deficient plasma cell infiltration in iMVI suggests an antibody-independent underlying stimulus. Additionally, iMVI shows decreased circulating T and NK cells, potentially due to their recruitment towards the graft endothelium.

What impact this may have on practice or policy: understanding the pathophysiological pathways of ABMR- and iMVI-damage should lead to improving diagnostic stratification, cost-efficient therapeutic decisions and outcomes.

INTRODUCTION

Antibody-mediated rejection (ABMR) is a leading cause of graft loss in kidney transplantation (KT) with no curative treatment.[1–6] Human leukocyte antigen (HLA) donor-specific antibodies (DSA) may exert their function activating the complement cascade by binding to HLA expressed by allograft endothelium, resulting in peritubular capillary C4d deposition, immune cell activation, and microvascular inflammation (MVI). The presence of glomerulitis (g) and/or peritubular capillaritis (ptc) characterizes MVI lesions on allograft tissue and may occur in the absence of complement activation.[5,7]

Since the Banff consensus in 2001, three main criteria outline ABMR diagnosis:[8,9] serologic evidence of circulating HLA-DSA, compatible histology (i.e., acute tubular necrosis, MVI, among others), and evidence of antibody-endothelium interaction (i.e., $C4d^+$ staining in peritubular capillaries). For some years, incomplete phenotypes combining two out of three criteria were classified as "suspicious for ABMR" (sABMR).[9] In 2013, the classification allowed diagnosis of C4d-negative ABMR if moderate MVI (defined as g+ptc≥ 2, and hereinafter referred to as MVI) was present.[10,11] Of note, the 2017 classification incorporated C4d staining and intrarenal gene transcripts as surrogates for HLA-DSA in the serological criterion, and the sABMR category was eliminated.[12] The criteria for ABMR diagnosis were unchanged in 2019.[13] Therefore, the presence of MVI on allograft biopsy is currently the cornerstone of ABMR diagnosis.[10,12] However, a subset of patients develops this lesion in the absence of detectable HLA-DSA and peritubular endothelial C4d deposition,[14,15] revealing an orphan category in recent Banff classifications that has shown to be a negative prognostic indicator of graft survival, independently of the C4d or HLA-DSA status.[11,16–18]

The pathogenesis of ABMR has been linked to the activation of memory B cells or plasma cells, which can produce antibodies that target mismatched donor molecules. The role of T cells in humoral rejection has been scarcely evaluated except for T follicular helper cells.[19,20] Moreover,

ABMR-damage frequently shows marked infiltration of macrophages, neutrophils, and Natural Killer (NK) cells, associated with poor outcomes.[21–24] In fact, transcriptomic studies have identified a signature associated with NK cells in ABMR.[25–28] Previous studies have hypothesized that the contribution of NK cells to graft rejection may depend on their ability to exert antibody-dependent cell-mediated cytotoxicity through the FcγRIIIA receptor (CD16A) triggered by HLA-DSAs attached to their target cells.[29] FcγRIIIA displays a common functional dimorphism (valine/phenylalanine-158, rs396991) which might be capable of modifying the receptor affinity for IgG subclasses and modulating the activity of FcγRIIIA-expressing leukocytes.[30] Furthermore, evidence suggests that NK cells may also be activated in the absence of HLA-DSAs being responsible for MVI on renal allograft biopsies due to the lack of recognition of donor HLA class I molecules by their inhibitory receptors, known as "missing-self" activation, pointing out to possible alternative mechanisms of NK cell activation after transplantation.[31–33] Although NK cells seem to be involved in both ABMR and iMVI,[34] the contribution of other immune cells to iMVI is not well charted.

Here, we aim to describe the participation of immune cells that may differ between isolated MVI (iMVI) and ABMR, reflecting different pathophysiology. For this purpose, we analyzed: a) peripheral blood lymphocytes (PBL) and b) infiltrating immune cells in KT biopsies of patients diagnosed with iMVI, ABMR, and a control group.

METHODS

Study population and design

Observational cohort study considering all KT patients from Hospital del Mar with surveillance and clinically indicated allograft biopsies performed between 2006 and 2018. Those cases accomplishing the histomorphological diagnosis of ABMR and iMVI were included. ABMR diagnosis and MVI score were defined according to Banff criteria.[13] Each patient contributed with one biopsy, always considering the first episode of ABMR/MVI. All patients with normal histology or mild IFTA were included as controls. HLA-DSA determination was performed in serum samples contemporaneous with allograft biopsies (**Suppl. Methods**).

The final cohort included 221 KT patients (116 controls, 73 with ABMR, and 32 with iMVI). First, PBL distribution was assessed in 204 KT patients with available samples: 64 ABMR, 27 iMVI, and 113 control cases. Blood samples were collected contemporaneously with the allograft biopsy (± 1.2 [0.4 – 2.7] months). Second, the immunohistochemistry analysis was performed in a cohort of 51 patients that fulfilled the following criteria: 1) iMVI group: histological features of MVI without historical or current circulating HLA antibodies nor C4d deposition, and without concomitant borderline/T-cell mediated rejection (TCMR) changes or glomerulonephritis; 2) ABMR group: histological features of MVI with circulating HLA-DSA ± C4d deposition, and without concomitant borderline/TCMR changes or glomerulonephritis, and 3) Normal group: normal histology or mild IFTA without historical or current circulating HLA antibodies. Thirty-four out of the 51 patients had both PBL immunophenotyping and immunohistochemistry studies, while 17 patients had only immunohistochemistry. Histological lesions were evaluated and blindly scored by an expert pathologist according to the most recent Banff classification.[12] Cases of active ABMR not fulfilling the MVI score and cases of non-active chronic ABMR were excluded to avoid bias. After the diagnostic process, residual formalin-fixed and paraffin-embedded (FFPE) material was included for further immunohistochemical analysis.

Demographical, clinicopathological, and immunological data were collected until graft loss, death, or June/2021. Treatment after ABMR histology diagnosis was indicated in clinically significant ABMR or iMVI cases. Subclinical and chronic ABMR / iMVI cases received no specific immunosuppression treatment.

The Parc de Salut Mar Ethical Research Board (2020/9117/I) approved the study, and all patients gave written informed consent. Clinical and research activities being reported herein are consistent with the Principles of Istanbul and Helsinki Declarations. The study was conducted according to the the STrengthening the Reporting of OBservational studies in Epidemiology (STROBE) guidelines.[35]

Peripheral blood lymphocyte immunophenotypic analysis

Blood samples were obtained by venous puncture in EDTA tubes concurrently to renal allograft biopsies. Prospective immunophenotyping of fresh samples was performed by flow cytometry. Briefly, samples were pretreated with saturating concentrations of human aggregated immunoglobulins to block FcγR and then labeled with different antibody combinations, as previously described.[36,37] Samples were acquired with a FACSCanto™ II flow cytometer, and data were analyzed by FACSDiva™ v.7 and FlowJo v.10 software (BD Biosciences™, NJ, USA). T cells were characterized as $CD3^+$ cells, and $CD4^+$, $CD8^+$, T regulatory ($CD25^{hi}$ $CD127^{neg/lo}$), and $\gamma\delta^+$ cell subsets were identified. B cells were characterized as $CD19^+$ cells, and naïve and memory B cell subsets were analyzed considering IgD and CD27 expression.[38] NK cells were defined as $CD3^-$ $CD56^+$ cells, and $CD56^{bright/dim}$, and NKG2A subsets were evaluated. Absolute cell numbers were calculated from parallel blood counts.

Immunohistochemical assessment

Three μm-thick sections were cut from one core FFPE tissue of a 16-gauge needle biopsy and stained using antibodies against CD3 (clone 2GV6, Roche, Switzerland), CD4 (clone SP35, Roche, Switzerland), CD8 (clone SP57, Roche Switzerland), CD20 (clone L26, Roche, Switzerland), CD68 (clone PGM1, Diagnostic Biosystems, Pleasanton, CA), CD56 (clone MRQ42, Roche, Switzerland), CD138 (clone B-A38, Roche, Switzerland) and TIA1 (2G9A10F5, Vitro Máster Diagnóstica, Granada, Spain). Here, TIA1 marker was used as a surrogate marker of cytotoxic T and NK cell granules.[39,40] Immunostains were automatically performed with a Benchmark XT (Roche, Switzerland) and revealed with DAB Optiview Kit (clone B-A38, Roche, Switzerland). Stained inflammatory cells were quantitatively assessed by two pathologists blinded for clinical background under light microscopy in the glomerular capillaries, peritubular capillaries, and interstitial compartment, especially when forming aggregates in scarred areas. A standardized evaluation of the cell count in renal parenchyma was conducted according to renal compartments. In glomerular capillaries, cell count was standardized by dividing the number of cells by the total glomeruli. In peritubular capillaries and renal interstitial compartments, cell count was standardized by dividing the number of cells by the length of the sample in millimeters.

CD16A (*FCGR3A*) 158 V/F genotyping

DNA from KT recipients of the immunohistochemical cohorts was isolated from total blood samples using the PureGene Blood Core Kit B (Qiagen). Functional polymorphisms of CD16A 158 V/F (FcγRIIIA) were determined using a PCR with confronting two-pair primers as previously described.[41]

Statistical analysis

According to their distribution, continuous data are presented as mean ± standard deviation (SD) or median and interquartile range (IQR). Categorical data are expressed as percentages. Comparison

of continuous variables between two or more groups was performed by *t*-test or ANOVA for parametric data and Mann-Whitney U-test or Kruskal-Wallis test for non-parametric distributions. Chi^2 or Fisher's exact tests, where appropriate, were used to compare nominal variables. Heatmap of Polyserial correlation was used to characterize inter-variable relationships. Survival analyses were performed using the Kaplan-Meier method using the log-rank test. Statistical analysis was performed using SPSS® Inc. statistics software v.28.0 and R v.4.0.5. A *p*-value <0.05 was considered statistically significant. For data presentation, we used GraphPad Prism software v.9.1.1.

RESULTS

Clinicopathologic description and graft survival

Patients' characteristics are shown in **Tables 1** and **2**. ABMR conferred the worst 5-year death-censored graft survival after biopsy among groups (ABMR: 63% vs. iMVI: 77% vs. Normal: 93%; $p<0.001$) (**Figure S1**).

Peripheral blood lymphocyte subset distribution

Table S1 summarizes PBL distribution data. The iMVI group presented lower total lymphocyte counts than Normal group (1662±828 vs. 2155±823 cells/μl) and ABMR group (vs. 2086±882 cells/μl).

iMVI diagnosis associates with lower counts of peripheral blood T cells

ABMR cases presented with a higher percentage of T cells (79.4±9.4%) compared with both iMVI and Normal groups (75.2±10% and 76.5±10%) (**Figure 1A**). Regarding total absolute counts, iMVI cases showed lower number of T cells than ABMR or Normal cases (1273±702 vs. 1675±746 or 1659±689 cells/μl, **Figure 1B**), parallel to lower total lymphocyte counts. We did not observe significant differences in the percentages of T $CD4^+$ and $CD8^+$ (**Figure 1C, E**). iMVI cases showed a significantly lower number of $CD4^+$ T cells compared with Normal cases (687±512 vs. 891±418 cells/μl) and of $CD8^+$ T cells compared with ABMR cases (532±251 vs. 739±403 cells/μl) (**Figure 1D, F**). No significant differences were observed in the ratio of $CD4^+/CD8^+$ T cells or T regulatory cells. We detected lower $\gamma\delta^+$ T cell numbers in iMVI vs. ABMR cases (**Figure S2A-B**).

Peripheral blood B cells distribution is similar between ABMR, iMVI, and Normal cases

The proportion and the absolute number of total B cells, naïve, and memory B cells were comparable between groups (**Figure S3A-F**).

ABMR and iMVI diagnoses relate to decreased circulating NK cells

ABMR cases presented lower percentages of circulating NK cells than Normal cases (10.1±7.7% vs. 13.1±7.7%) (**Figure 2A**). The absolute number of circulating NK cells appeared reduced in both ABMR and iMVI cases compared to controls (198±156 and 201±155 vs. Normal 283±203 cells/μl) (**Figure 2B**). We found a higher percentage of $NKG2A^+$ NK cells restricted to ABMR cases compared with Normal biopsies (51.3±20% vs. 44.4±17.7%) (**Figure 2C, E**). $NKG2A^+$ NK absolute cell numbers were lower in both iMVI and ABMR compared to Normal biopsies (iMVI 65±47 and ABMR 98±98 vs. Normal: 117±93 cells/μl) (**Figure 2D**). However, only ABMR patients presented lower numbers of $NKG2A^-$ NK cells compared to the Normal group (100±95 vs. 166±144 cells/μl) (**Figure 2F**). Both ABMR and iMVI groups showed decreased numbers of circulating $CD56^{dim}$ NK cells compared with Normal cases (ABMR: 190±155 and iMVI: 188±158 cells/μl vs. Normal: 269±201 cells/μl), but similar numbers of the $CD56^{bright}$ subset (**Figure S4A-D**).

Immunohistochemical assessment in KT biopsies

The immunohistochemical assessment was performed in 51 patients, including 22 ABMR, 13 iMVI, and 16 Normal biopsies (**Figure S5A-H**). Baseline and clinicopathological characteristics are summarized in **Tables S2** and **S3**.

Glomerular compartment

ABMR and iMVI patients showed more $CD3^+$ cell infiltration in the glomerular compartment than the Normal group (4.6±4.6 and 6.5±6.2 vs. 1.1±0.9 cells/glomerulus, respectively, **Figure 3A**). This increase was on account of both $CD4^+$ and $CD8^+$ cells in iMVI patients and predominantly due to $CD4^+$ infiltrates in the ABMR group (**Figure 3B-C**). There were no $CD20^+$ cell infiltration differences between groups (**Figure 3D**). Patients with ABMR and iMVI had more intense $CD68^+$ infiltration than the Normal group (4.5±3.5 and 3.5±2.8 vs. 1.0±1.2 cells/glomerulus, **Figure 3E**). Otherwise, $CD56^+$ cell infiltration was similar (**Figure 3F**). We next investigated the presence of

cytotoxic cells in the glomerular compartment using the TIA1 marker, expressed in both $CD8^+$ T lymphocytes and NK cells.[42] iMVI patients displayed a significant increase of $TIA1^+$ lymphocytes compared with the Normal group, in line with T lymphocyte infiltration. Moreover, a non-significant increase in $TIA1^+$ cells was also perceived in iMVI compared to ABMR (**Figure 3G**).

Peritubular capillary compartment

Peritubular capillaries displayed more $CD3^+$ cells in ABMR and iMVI groups (19.6±8.9 and 23.3±11.1 vs. 9.9±6.1 cells in ptc/mm^2 of tissue, **Figure 4A**), as well as more $CD4^+$ and $CD8^+$ cells compared to the Normal group (**Figure 4B-C**). B cell distribution ($CD20^+$ cells) appeared similar between the three groups (**Figure 4D**). More $CD68^+$ cells (ABMR: 12.8±9.9 and iMVI: 9.5±7.2 vs. Normal: 3.2±3.7 cells in ptc/mm^2 of tissue) and $CD56^+$ cells (ABMR: 1.7±1.5 and iMVI: 1.7±1.7 vs. Normal: 0.2 ± 0.3 cells in ptc/mm^2 of tissue) were observed in ABMR and iMVI patients (**Figure 4E-F)**. Increased $TIA1^+$ cells were observed in ABMR and iMVI compared to the Normal group, in line with increased $CD3^+$ and $CD56^+$ cells (**Figure 4G**). Moreover, more plasma cells ($CD138^+$) were observed in ABMR patients compared to iMVI and Normal groups (ABMR: 1.0±1.6 vs. iMVI: 0.3±0.5 and Normal: 0.2±0.2 cells in ptc/mm^2 of tissue, **Figure 4H**).

Cortical interstitial compartment (interstitial aggregates)

We observed no significant differences between groups regarding $CD3^+$, $CD20^+$, $CD68^+$, $CD56^+$ and $TIA1^+$ infiltration in interstitial aggregates (**Figure 5A-G**). However, the interstitial compartment displayed a significantly greater plasma cell infiltration in ABMR than iMVI patients (1.9±1.9 vs. 0.7±1.3 cells /mm^2 of tissue, **Figure 5H**).

Since post-transplant time to allograft biopsy differed between ABMR and iMVI groups (Table S2), we performed a regression analysis studying the impact of this variable on cell infiltrates in the different renal compartments. Of note, time after KT showed no impact on the number of CD8+ and TIA1+ cells in the glomeruli (adjusted R-squared: -0.014 and -0.022, respectively) or CD138+ in

peritubular capillaries and interstitial aggregates (adjusted R-squared: 0.016 and -0.009, respectively) in our limited cohort.

Leukocyte infiltration distribution and FcγRIIIA 158 F/V polymorphisms

Analysis of the relation between FcγRIIIA 158 F/V polymorphism and leukocyte infiltration revealed that in cases with ABMR-histology, the 158-V-carrier genotype was associated with increased glomerular $CD3^+$ (6.3±6.1 vs. 3.4±1.8, p=0.051) and $CD8^+$ cell infiltration (3.9±4.9 vs. 1.7±1.2, p=0.050), compared to recipients with the 158-F/F-genotype (**Table S4**).

Topographical leukocyte infiltration and histologic features

In the heatmap of Polyserial correlation between topographical standardized leukocyte infiltration and the severity of histologic lesions, $CD3^+$, $CD4^+$, $CD8^+$, and $CD56^+$ cells were strongly associated with the severity of glomerulitis and peritubular capillaritis in iMVI cases, whereas $CD68^+$ infiltrates were only associated with the severity of glomerulitis (**Figure 6**). The ABMR group showed a correlation between glomerular leukocyte infiltrates and glomerulitis intensity. Contrariwise, any specific leukocyte subset infiltrates within the ptc in ABMR showed a strong correlation with the severity of ptc. Glomerular leukocyte infiltration was inversely correlated with chronic changes such as IFTA or transplant glomerulopathy in the iMVI group, while IFTA was increased in ABMR cases with glomerular leukocyte infiltration.

DISCUSSION

MVI histology without evidence of circulating HLA-DSA and without endothelial C4d deposition has become an orphan category in recent Banff classifications. We aimed to better understand the topographical immune cell infiltration in iMVI and ABMR cases. We demonstrated major leukocyte infiltrate alterations in biopsy specimens with iMVI, showing intense T cell and NK cell cytotoxic phenotypes, like ABMR. Interestingly, $CD8^+$ T cells appear to be the predominant cytotoxic cells involved in glomerular infiltration in iMVI. Besides, the lack of plasma cell infiltration in iMVI supports a distinct pathophysiological damage mechanism. Complementarily, peripheral blood immune cell distribution displayed decreased global T and NK cell counts in iMVI cases, potentially resulting from increased binding of immune cells in the graft endothelium.

Updates to the Banff classification have attempted to better categorize the phenotypic expressions of ABMR over time.[8,10,12,13,43] With C4d deposition as a surrogate for DSA, the sABMR category was removed in the Banff 2017 revision, and MVI lesions without DSA or C4d deposition were no longer included in category 2.[12] Recent data assessing the impact and risk stratification of the proposed changes point that a binary classification system inadequately represents the clinical and histological heterogeneity of ABMR.[34,44] Indeed, iMVI lesions have shown an intermediate prognosis compared with ABMR cases and non-ABMR histology,[15,44–46] similar to what we observed in the present study.

Increased recognition of serological and histological ABMR heterogeneity has led researchers to seek new diagnostic and prognostic biomarkers. Several groups have investigated the association between PBL subpopulations and KT outcomes, particularly ABMR or HLA-DSA development. On that account, patients with chronic ABMR have shown increased numbers of circulating $CD8^+$ $CD28^-$ T lymphocytes compared with cases of graft tolerance.[47] Furthermore, Louis *et al.* recently identified highly coordinated circulating T follicular helper cells and activated B cells among patients with ABMR, in contrast with patients who did not develop HLA-DSAs or ABMR.[48] When

comparing ABMR-histology with and without HLA-DSA and C4d deposition, we observed a selective depletion of peripheral $CD8^+$ T lymphocytes in the iMVI group compared to full-ABMR diagnosis and reduced circulating $CD4^+$ T lymphocytes and NK cells compared to normal cases. The depletion of circulating immune cell populations in patients with iMVI may be attributed to the increased binding of immune cells to the allograft endothelium.[49] This correlates with the greater T cell infiltration observed in the tissue in iMVI cases compared with the normal group, despite similar infiltration in ABMR.

Concerning circulating NK cells, we previously reported an association between HLA-DSA and higher proportions of $CD56^{bright}$ and $CD56^{dim}$ $NKG2A^+$ subsets, together with a lower percentage of $CD56^{dim}$ NK cells, especially in HLA-DSA recipients with ABMR.[50] Similarly, Neudoerfl *et al.* reported reduced numbers of $CD56^{dim}$ NK subset in HLA-DSA patients compared with cases without HLA antibodies.[51] Our data now show an increased proportion of circulating $NKG2A^+$ NK cells in ABMR compared to normal cases, encompassed by a reduction in the proportion of $NKG2A^-$ NK cells. $NKG2A^+$ NK cell numbers appeared reduced in both ABMR and iMVI groups, consistent with a lower absolute number of $CD56^{dim}$ NK cells. Interestingly, $NKG2A^-$ NK cell numbers were diminished only in ABMR cases, suggesting a selective depletion of this NK cell subset. While several hypotheses have been proposed concerning the etiopathology of iMVI cases,[34] the limited impact of MVI-damage on NK cell subsets distribution, compared with the remarkable impact of ABMR, favors the hypothesis of a CD16A-independent NK cell "missing self-activation" mechanism in the former group.[31–33,45] As this mechanism would involve only alloreactive NK cell subsets governed by inhibitory KIR mismatched with graft HLA class I molecules, a potential impact on the total circulating NK cell compartment distribution would be minimized.

Assessing allograft inflammatory infiltrates provides a more precise diagnosis and pathophysiologic approach than conventional histology alone. Most transcriptomic studies of ABMR biopsies have reported an immune cell infiltrate scenario hallmarked by $CD8^+$ T cells, monocytes/macrophages,

279 and NK cells.[45,52–54] This immune cell landscape is consistent with our findings from the
280 immunohistochemical analysis. Despite the attractiveness of molecular markers due to their high
281 reproducibility,[55] alternative approaches such as immunostaining or multiplex immunofluorescent
282 staining reveal the association between leukocyte populations and their intragraft location, adding
283 more pieces to the puzzle.[45,56] Indeed, others have studied inflammatory infiltrate components over
284 time or their relationship with outcomes,[7,57] which may be crucial for future targeted therapies. Our
285 study identified an intense expression of the T and NK cell cytotoxic marker TIA-1 in iMVI cases,
286 like in ABMR. Of interest, albeit ABMR and iMVI groups displayed a heightened T cell component
287 into the microvascular compartments compared to controls, iMVI reflected a more pronounced
288 $CD8^+$ and $TIA1^+$ glomeruli infiltration tendency than ABMR, which may correlate with the
289 decreased peripheral blood T cells. Consistently, Sablik *et al.* also found a predominance of T cell
290 infiltrates (particularly $CD8^+$) in the glomeruli.[58] These findings highlight the role of T cells in the
291 pathophysiology of MVI lesions, irrespective of HLA-DSA status, which should be further
292 characterized. Additionally, ptc displayed more $CD56^+$ cells in ABMR and iMVI cases than
293 controls, contrarily to the glomeruli. Remarkably, $CD56^+$ infiltration was only associated with the
294 severity of peritubular capillaritis in iMVI cases. Contrariwise, others have described a strong
295 correlation between NK cells and the severity of all microcirculation components in patients with
296 MVI irrespective of HLA-DSA status.[45,56] Moreover, Callemeyn *et al.* found similar upregulation
297 of pathways and enrichment of infiltrating leucocytes in patients with ABMR histology with and
298 without HLA-DSA.[45] Anyhow, the authors defined MVI as $g+ptc \geq 1$, and $C4d^+$ cases were also part
299 of the ABMR-histology $HLA\text{-}DSA^-$ diagnosis, so these results cannot be directly compared with
300 ours. Due to the heterogeneity of NK cell subsets, phenotypic markers of NK cells should be further
301 evaluated in renal tissue. In fact, Jung *et al.* identified $CD56^+CD57^+$ infiltrates as the most frequently
302 subset observed in ABMR compared to TCMR.[24] This phenotype is associated with the terminal
303 differentiation of cells that display potent effector functions.[24,59]

The fact that T cells and macrophages predominate in glomerulitis and NK cells in ptc damage may be of relevance to look for targeted drugs. More importantly, our data suggest that the lack of plasma cell tissue infiltration in iMVI cases compared to ABMR, together with the absence of HLA-DSA and complement activation, could imply a distinct pathophysiological damage mechanism, possibly antibody-independent (**Figure 7**). Although plasma cell infiltration has been correlated with time after transplantation in previous studies,[60] our regression analysis ruled out this effect in our cohort. In line with this assumption, other groups have demonstrated that NK cell activation through missing self was an antibody-independent stimulus for microvascular inflammation.[31–33,45]

Regarding the FcγRIIIA 158 F/V polymorphism data, our KT recipients with ABMR-histology and at least one valine allele displayed higher $CD3^+$, $CD8^+$, and $CD56^+$ infiltration than those without valine, which merits further assessment. Considering that most T-cells do not express CD16, these results could mirror an increased number of $\gamma\delta^+$ T cells (which do express CD16) infiltrating in ABMR-histology cases.[61,62] In fact, we observed a significant reduction of peripheral blood $\gamma\delta^+$ T cells in iMVI cases. We cannot exclude the possibility that ABMR-damage may imply a significant increase of $CD8^+$ T cells expressing CD16, which has been observed in other pathological situations.[63]

This study has several limitations. First, we did not assess non-HLA antibodies or transcriptomic analysis in our cohort. Nonetheless, although some studies have found that the screening for circulating functional non-HLA antibodies may be clinically relevant (i.e., anti-AT1R antibodies)[64], our previously reported experience shows that most ABMR cases without HLA-DSA do not present the most classical non-HLA antibodies.[18] Second, the strict selection criteria of eligible KT recipients applied for the immunohistochemistry study limited the cohort size and disallowed performing paired-sample analysis according to post-transplant time. Third, colocalization studies in kidney tissue, i.e., $TIA1^+$, $CD8^+$, and NK, have not been performed. Fourth, the number of markers assessed by flow cytometry in peripheral blood was limited as the main objective was to

correlate these results with the topographical immune cell infiltration. Finally, further validation with external datasets will be necessary to support our findings.

In summary, our data demonstrate that KT recipients with MVI histology in the absence of HLA-DSA and C4d endothelial deposition display decreased circulating T cell and NK cells together with T and NK cell infiltration in the allograft, similar to ABMR. We found a distinct glomerular infiltration of cytotoxic CD8 T cells in iMVI. Besides, the scarce plasma cell infiltration in this group suggests a different underlying mechanism of damage compared to full-ABMR. Understanding the pathophysiological pathways of ABMR-histology with different phenotypic expressions may lead the transplant community to reconsider diagnostic stratification and more targeted treatments to improve long-term KT outcomes.

AUTHOR CONTRIBUTIONS

MC and JP designed the project. AB, LLM, and MC designed the specific study. AB, LLM, and DR-P participated in the acquisition of data. JG and AP revised and scored biopsy specimens. LLM and JY revised peripheral flow cytometry studies. LLM and CV performed the CD16A 158 V/F genotyping. AB and LLM analyzed the data and drafted the manuscript. DR-P, CA-C, CB, JY, ML-B, MN, MJP-S, JP, and MC participated in the critical revision of the manuscript for important intellectual content. All authors have read and approved the final manuscript.

ACKNOWLEDGMENTS

We thank Marisa Mir, Adriana Sierra, Alfonso Califano, Ana Marina Granados, Sheila Bermejo, Anna Faura, Montserrat Folgueiras, Maria Vera and Sara Álvarez for their contribution to the development of the TRASMAR database. We are indebted to Rosa Causadías, Anna Bach, Guillermo Pedreira and Aida Martínez for their assistance with patients. We thank Cristian Tebé for providing statistical support. We express our gratitude to Dulce Soto and Gemma Heredia for their technical help. AB did this study as part of her doctoral thesis program at the Department of Medicine from the Universitat Autonoma of Barcelona (UAB).

FUNDING

AB has support from a Rio Hortega contract (CM19/00004, ISCIII), a M-AES grant (MV20/00072, ISCIII), and a Spanish Society of Nephrology scholarship. This study was performed with funding from projects PI16/00619 and PI20/00090 (Spanish Ministry of Health ISCIII FIS-FEDER); RD16/0009/0013 (ISCIII FEDER REDinREN) and 201822-10 (Fundació la Marató de TV3). MC is partially supported by a grant from the Spanish Ministry of Health ISCIII FIS-FEDER INT21/0003.

DISCLOSURE

The authors declare no financial disclosures or conflicts of interest.

DATA AVAILABILITY STATEMENT

The data that support the findings of this study are available on request from the corresponding author. The data are not publicly available due to privacy or ethical restrictions.

REFERENCES

1. Einecke G, Sis B, Reeve J, et al. Antibody-mediated microcirculation injury is the major cause of late kidney transplant failure. *Am J Transplant*. 2009;9(11):2520-2531. doi:10.1111/j.1600-6143.2009.02799.x
2. Sellarés J, De Freitas DG, Mengel M, et al. Understanding the causes of kidney transplant failure: The dominant role of antibody-mediated rejection and nonadherence. *Am J Transplant*. 2012;12(2):388-399. doi:10.1111/j.1600-6143.2011.03840.x
3. Halloran PF, Chang J, Famulski K, et al. Disappearance of T cell-mediated rejection despite continued antibody-mediated rejection in late kidney transplant recipients. *J Am Soc Nephrol*. 2015;26(7):1711-1720. doi:10.1681/ASN.2014060588
4. Arias-Cabrales C, Redondo-Pachón D, Pérez-Sáez MJ, et al. Renal graft survival according to Banff 2013 classification in indication biopsies. *Nefrologia*. 2016;36(6):660-666. doi:10.1016/j.nefro.2016.05.018
5. Loupy A, Lefaucheur C. Antibody-Mediated Rejection of Solid-Organ Allografts. *N Engl J Med*. 2018;379(12):1150-1160. doi:10.1056/nejmra1802677
6. Van Loon E, Bernards J, Van Craenenbroeck AH, Naesens M. *The Causes of Kidney Allograft Failure: More than Alloimmunity. A Viewpoint Article*.; 2020. doi:10.1097/TP.0000000000003012
7. Delsante M, Maggiore U, Levi J, et al. Microvascular inflammation in renal allograft biopsies assessed by endothelial and leukocyte co-immunostain: a retrospective study on reproducibility and clinical/prognostic correlates. *Transpl Int*. 2019;32(3):300-312. doi:10.1111/tri.13371
8. Racusen LC, Colvin RB, Solez K, et al. Antibody-mediated rejection criteria - An addition to the Banff '97 classification of renal allograft rejection. *Am J Transplant*. 2003;3(6):708-714. doi:10.1034/j.1600-6143.2003.00072.x

9. Haas M. An updated Banff schema for diagnosis of antibody-mediated rejection in renal allografts. *Curr Opin Organ Transplant*. 2014;19(3):315-322. doi:10.1097/MOT.0000000000000072

10. Haas M, Sis B, Racusen LC, et al. Banff 2013 meeting report: Inclusion of C4d-negative antibody-mediated rejection and antibody-associated arterial lesions. *Am J Transplant*. 2014;14(2):272-283. doi:10.1111/ajt.12590

11. Loupy A, Hill GS, Suberbielle C, et al. Significance of C4d Banff scores in early protocol biopsies of kidney transplant recipients with preformed donor-specific antibodies (DSA). *Am J Transplant*. 2011;11(1):56-65. doi:10.1111/j.1600-6143.2010.03364.x

12. Haas M, Loupy A, Lefaucheur C, et al. The Banff 2017 Kidney Meeting Report: Revised diagnostic criteria for chronic active T cell–mediated rejection, antibody-mediated rejection, and prospects for integrative endpoints for next-generation clinical trials. *Am J Transplant*. 2018;18(2):293-307. doi:10.1111/ajt.14625

13. Loupy A, Haas M, Roufosse C, et al. The Banff 2019 Kidney Meeting Report (I): Updates on and clarification of criteria for T cell– and antibody-mediated rejection. *Am J Transplant*. 2020;20(9):2318-2331. doi:10.1111/ajt.15898

14. Delville M, Lamarthée B, Pagie S, et al. Early acute microvascular kidney transplant rejection in the absence of anti-HLA antibodies is associated with preformed IgG antibodies against diverse glomerular endothelial cell antigens. *J Am Soc Nephrol*. 2019;30(4):692-709. doi:10.1681/ASN.2018080868

15. Senev A, Coemans M, Lerut E, et al. Histological picture of antibody-mediated rejection without donor-specific anti-HLA antibodies: Clinical presentation and implications for outcome. *Am J Transplant*. 2019;19(3):763-780. doi:10.1111/ajt.15074

16. Sis B, Jhangri GS, Riopel J, et al. A new diagnostic algorithm for antibody-mediated microcirculation inflammation in kidney transplants. *Am J Transplant*. 2012;12(5):1168-

1179. doi:10.1111/j.1600-6143.2011.03931.x

17. Parajuli S, Redfield RR, Garg N, et al. Clinical significance of microvascular inflammation in the absence of anti-HLA DSA in kidney transplantation. *Transplantation*. 2019;103(7):1468-1476. doi:10.1097/TP.0000000000002487

18. Crespo M, Llinàs-Mallol L, Redondo-Pachón D, et al. Non-HLA Antibodies and Epitope Mismatches in Kidney Transplant Recipients With Histological Antibody-Mediated Rejection. *Front Immunol*. 2021;12(July):1-12. doi:10.3389/fimmu.2021.703457

19. Louis K, Macedo C, Lefaucheur C, Metes D. Adaptive immune cell responses as therapeutic targets in antibody-mediated organ rejection. *Trends Mol Med*. 2022;28(3):237-250. doi:10.1016/j.molmed.2022.01.002

20. Benedetti Gassen R, Borges T, Pérez-Sáez M, et al. T cell depletion increases humoral response by favoring T follicular helper cells expansion. *Am J Transplant*. Published online 2022:[Online ahead of print]. doi:10.1111/ajt.17038

21. Lefaucheur C, Nochy D, Hill GS, et al. Determinants of poor graft outcome in patients with antibody-mediated acute rejection. *Am J Transplant*. 2007;7(4):832-841. doi:10.1111/j.1600-6143.2006.01686.x

22. Magil AB. Monocytes/macrophages in renal allograft rejection. *Transplant Rev*. 2009;23(4):199-208. doi:10.1016/j.trre.2009.06.005

23. Valenzuela NM, Trinh KR, Mulder A, Morrison SL, Reed EF. Monocyte recruitment by HLA IgG-activated endothelium: The relationship between IgG subclass and FcγRIIa polymorphisms. *Am J Transplant*. 2015;15(6):1502-1518. doi:10.1111/ajt.13174

24. Jung HR, Kim MJ, Wee YM, et al. CD56+CD57+ infiltrates as the most predominant subset of intragraft natural killer cells in renal transplant biopsies with antibody-mediated rejection. *Sci Rep*. 2019;9(1):1-10. doi:10.1038/s41598-019-52864-5

25. Hidalgo LG, Sis B, Sellares J, et al. NK cell transcripts and NK cells in kidney biopsies from

patients with donor-specific antibodies: Dvidence for NK cell involvement in antibody-mediated rejection. *Am J Transplant*. 2010;10(8):1812-1822. doi:10.1111/j.1600-6143.2010.03201.x

26. Hidalgo LG, Sellares J, Sis B, Mengel M, Chang J, Halloran PF. Interpreting NK cell transcripts versus T cell transcripts in renal transplant biopsies. *Am J Transplant*. 2012;12(5):1180-1191. doi:10.1111/j.1600-6143.2011.03970.x

27. Kohei N, Tanaka T, Tanabe K, et al. Natural killer cells play a critical role in mediating inflammation and graft failure during antibody-mediated rejection of kidney allografts. *Kidney Int*. 2016;89(6):1293-1306. doi:10.1016/j.kint.2016.02.030

28. Yazdani S, Callemeyn J, Gazut S, et al. Natural killer cell infiltration is discriminative for antibody-mediated rejection and predicts outcome after kidney transplantation. *Kidney Int*. 2019;95(1):188-198. doi:10.1016/j.kint.2018.08.027

29. Parkes MD, Halloran PF, Hidalgo LG. Evidence for CD16a-Mediated NK Cell Stimulation in Antibody-Mediated Kidney Transplant Rejection. *Transplantation*. 2017;101(4):e102-e111. doi:10.1097/TP.0000000000001586

30. Bruhns P, Iannascoli B, England P, et al. Specificity and affinity of human Fcγ receptors and their polymorphic variants for human IgG subclasses. *Blood*. 2009;113(16):3716-3725. doi:10.1182/blood-2008-09-179754

31. Koenig A, Chen CC, Marçais A, et al. Missing self triggers NK cell-mediated chronic vascular rejection of solid organ transplants. *Nat Commun*. 2019;10(1). doi:10.1038/s41467-019-13113-5

32. Callemeyn J, Senev A, Coemans M, et al. Missing Self–Induced Microvascular Rejection of Kidney Allografts: A Population-Based Study. *J Am Soc Nephrol*. 2021;32(8):2070-2082. doi:10.1681/asn.2020111558

33. Koenig A, Mezaache S, Callemeyn J, et al. Missing Self-Induced Activation of NK Cells

Combines with Non-Complement-Fixing Donor-Specific Antibodies to Accelerate Kidney Transplant Loss in Chronic Antibody-Mediated Rejection. *J Am Soc Nephrol*. 2021;32(2):479-494. doi:10.1681/ASN.2020040433

34. Callemeyn J, Lamarthée B, Koenig A, Koshy P, Thaunat O, Naesens M. Allorecognition and the spectrum of kidney transplant rejection. *Kidney Int*. 2022;101(4):692-710. doi:10.1016/j.kint.2021.11.029

35. Von Elm E, Altman DG, Egger M, Pocock SJ, Gøtzsche PC, Vandenbrouckef JP. The Strengthening the Reporting of Observational Studies in Epidemiology (STROBE) Statement: Guidelines for reporting observational studies. *Bull World Health Organ*. 2007;85(11):867-872. doi:10.2471/BLT.07.045120

36. Llinàs-Mallol L, Redondo-Pachón D, Pérez-Sáez MJ, et al. Peripheral blood lymphocyte subsets change after steroid withdrawal in renal allograft recipients: a prospective study. *Sci Rep*. 2019;9(1):1-11. doi:10.1038/s41598-019-42913-4

37. Llinàs-Mallol L, Redondo-Pachón D, Raïch-Regué D, et al. Long-Term Redistribution of Peripheral Lymphocyte Subpopulations after Switching from Calcineurin to mTOR Inhibitors in Kidney Transplant Recipients. *J Clin Med*. 2020;9(4):1088. doi:10.3390/jcm9041088

38. Sanz I, Wei C, Lee FEH, Anolik J. Phenotypic and functional heterogeneity of human memory B cells. *Semin Immunol*. 2008;20(1):67-82. doi:10.1016/j.smim.2007.12.006

39. Tian Q, Streuli M, Saito H, Schlossman SF, Anderson P. A polyadenylate binding protein localized to the granules of cytolytic lymphocytes induces DNA fragmentation in target cells. *Cell*. 1991;67(3):629-639. doi:10.1016/0092-8674(91)90536-8

40. Kawakami A, Tian Q, Duan X, Streuli M, Schlossman SF, Anderson P. Identification and functional characterization of a TIA-1-related nucleolysin. *Proc Natl Acad Sci USA*. 1992;89(18):8681-8685.

41. Vilches C, Castaño J, Muñoz P, Peñalver J. Simple genotyping of functional polymorphisms of the human immunoglobulin G receptors CD16A and CD32A: A reference cell panel. *Tissue Antigens*. 2008;71(3):242-246. doi:10.1111/j.1399-0039.2007.00998.x

42. Anderson P, Nagler-Anderson C, O'Brien C, et al. A monoclonal antibody reactive with a 15-kDa cytoplasmic granule-associated protein defines a subpopulation of CD8+ T lymphocytes. *J Immunol*. 1990;144(2):574–582.

43. Loupy A, Mengel M, Haas M. 30 years of the International Banff Classification for Allograft Pathology: The Past, Present and Future of Kidney Transplant Diagnostics. *Kidney Int*. Published online 2021. doi:10.1016/j.kint.2021.11.028

44. Callemeyn J, Ameye H, Lerut3 E, et al. Revisiting the Changes in the Banff Classification for Antibody-Mediated Rejection after Kidney Transplantation. *Am J Transplant*. 2021;21(7):2413-2423. doi:10.1111/ajt.16474

45. Callemeyn J, Lerut E, de Loor H, et al. Transcriptional Changes in Kidney Allografts with Histology of Antibody-Mediated Rejection without Anti-HLA Donor-Specific Antibodies. *J Am Soc Nephrol*. 2020;31(9):2168-2183. doi:10.1681/ASN.2020030306

46. Coemans M, Senev A, Van Loon E, et al. The evolution of histological changes suggestive of antibody-mediated injury, in the presence and absence of donor-specific anti-HLA antibodies. *Transpl Int*. 2021;34(10):1824-1836. doi:10.1111/tri.13964

47. Baeten D, Louis S, Braud C, et al. Phenotypically and functionally distinct CD8+ lymphocyte populations in long-term drug-free tolerance and chronic rejection in human kidney graft recipients. *J Am Soc Nephrol*. 2006;17(1):294-304. doi:10.1681/ASN.2005020178

48. Louis K, Macedo C, Bailly E, et al. Coordinated circulating T follicular helper and activated B cell responses underlie the onset of antibody-mediated rejection in kidney transplantation. *J Am Soc Nephrol*. 2020;31(10):2457-2474. doi:10.1681/ASN.2020030320

49. Cross AR, Glotz D, Mooney N. The role of the endothelium during Antibody-mediated

520 rejection: From victim to accomplice. *Front Immunol*. 2018;9(JAN):1-7.
521 doi:10.3389/fimmu.2018.00106
522 50. Crespo M, Yelamos J, Redondo D, et al. Circulating NK-cell subsets in renal allograft
523 recipients with anti-HLA donor-specific antibodies. *Am J Transplant*. 2015;15(3):806-814.
524 doi:10.1111/ajt.13010
525 51. Neudoerfl C, Mueller BJ, Blume C, et al. The peripheral NK cell repertoire after kidney
526 transplantation is modulated by different immunosuppressive drugs. *Front Immunol*.
527 2013;4(FRB):1-14. doi:10.3389/fimmu.2013.00046
528 52. Sellarés J, Reeve J, Loupy A, et al. Molecular diagnosis of antibody-mediated rejection in
529 human kidney transplants. *Am J Transplant*. 2013;13(4):971-983. doi:10.1111/ajt.12150
530 53. Halloran PF, Pereira AB, Chang J, et al. Microarray diagnosis of antibody-mediated rejection
531 in kidney transplant biopsies: An international prospective study (INTERCOM). *Am J*
532 *Transplant*. 2013;13(11):2865-2874. doi:10.1111/ajt.12465
533 54. Venner JM, Hidalgo LG, Famulski KS, Chang J, Halloran PF. The molecular landscape of
534 antibody-mediated kidney transplant rejection: Evidence for NK involvement through CD16a
535 Fc receptors. *Am J Transplant*. 2015;15(5):1336-1348. doi:10.1111/ajt.13115
536 55. Mengel M, Loupy A, Haas M, et al. Banff 2019 Meeting Report: Molecular diagnostics in
537 solid organ transplantation–Consensus for the Banff Human Organ Transplant (B-HOT) gene
538 panel and open source multicenter validation. *Am J Transplant*. 2020;20(9):2305-2317.
539 doi:10.1111/ajt.16059
540 56. Calvani J, Terada M, Lesaffre C, et al. In situ multiplex immunofluorescence analysis of the
541 inflammatory burden in kidney allograft rejection: A new tool to characterize the alloimmune
542 response. *Am J Transplant*. 2020;20(4):942-953. doi:10.1111/ajt.15699
543 57. Aguado-Domínguez E, Cabrera-Pérez R, Suarez-Benjumea A, Abad-Molina C, Núñez-
544 Roldán A, Aguilera I. Computer-Assisted Definition of the Inflammatory Infiltrates in

Patients With Different Categories of Banff Kidney Allograft Rejection. *Front Immunol*. 2019;10(November). doi:10.3389/fimmu.2019.02605

58. Sablik KA, Jordanova ES, Pocorni N, Clahsen-van Groningen MC, Betjes MGH. Immune Cell Infiltrate in Chronic-Active Antibody-Mediated Rejection. *Front Immunol*. 2020;10(February):1-8. doi:10.3389/fimmu.2019.03106

59. Kared H, Martelli S, Ng TP, Pender SLF, Larbi A. CD57 in human natural killer cells and T-lymphocytes. *Cancer Immunol Immunother*. 2016;65(4):441-452. doi:10.1007/s00262-016-1803-z

60. Einecke G, Reeve J, Mengel M, et al. Expression of B cell and immunoglobulin transcripts is a feature of inflammation in late allografts. *Am J Transplant*. 2008;8(7):1434-1443. doi:10.1111/j.1600-6143.2008.02232.x

61. Couzi L, Pitard V, Sicard X, et al. Antibody-dependent anti-cytomegalovirus activity of human γδ T cells expressing CD16 (FcγRIIIa). *Blood*. 2012;119(6):1418-1427. doi:10.1182/blood-2011-06-363655

62. Lawand M, Déchanet-Merville J, Dieu-Nosjean MC. Key features of gamma-delta T-cell subsets in human diseases and their immunotherapeutic implications. *Front Immunol*. 2017;8(JUN). doi:10.3389/fimmu.2017.00761

63. Björkström NK, Gonzalez VD, Malmberg K-J, et al. Elevated Numbers of FcγRIIIA + (CD16 +) Effector CD8 T Cells with NK Cell-Like Function in Chronic Hepatitis C Virus Infection . *J Immunol*. 2008;181(6):4219-4228. doi:10.4049/jimmunol.181.6.4219

64. Lefaucheur C, Viglietti D, Bouatou Y, et al. Non-HLA agonistic anti-angiotensin II type 1 receptor antibodies induce a distinctive phenotype of antibody-mediated rejection in kidney transplant recipients. *Kidney Int*. 2019;96(1):189-201. doi:10.1016/j.kint.2019.01.030

Table 1. Demographic and clinicopathological characteristics of the study population.

	Normal (n=116)	ABMR (n=73)	iMVI (n=32)	p-value 3 groups	p-value ABMR vs. iMVI
At transplantation					
Recipient age, years, mean ± SD	53 ± 13	49 ± 15	57 ± 14	**0.019**	**0.012**
Recipient sex female, n (%)	44 (37.9)	29 (39.7)	18 (56.3)	0.170	0.139
Type of donor (deceased), n (%)	95 (81.9)	70 (95.9)	24 (75)	**0.003**	**0.003**
Donor age, years, mean ± SD	55 ± 16	48 ± 19	58 ± 13	**0.003**	**0.002**
Retransplantation, n (%)	13 (11.2)	15 (20.5)	1 (3.1)	**0.043**	**0.035**
Pretransplant HLA-DSA, n (%) (n=206)	11 (9.6)	22 (34.9)	2 (6.9)	**<0.001**	**0.004**
HLA-A/B/DR mismatch, mean (SD)	4 ± 1.2	4.4 ± 1.2	4.1 ± 1.5	0.275	0.588
CMV status, n (%) D^-/R^- D^-/R^+ D^+/R^- D^+/R^+	 7 (6) 12 (10.3) 10 (8.6) 87 (75)	 3 (4.2) 9 (12.7) 8 (11.3) 51 (71.8)	 0 (0) 3 (9.4) 2 (6.3) 27 (84.4)	0.747	0.459
Thymoglobulin induction, n (%)	13 (11.2)	23 (31.5)	7 (21.9)	**0.001**	0.307
Calcineurin inhibitors, n (%)	116 (100)	73 (100)	32 (100)	1.000	1.000
Mycophenolic acid, n (%)	105 (90.5)	57 (78.1)	22 (68.8)	**0.005**	0.333
mTOR inhibitors, n (%)	10 (8.6)	13 (17.8)	10 (31.3)	**0.005**	0.199
Clinical characteristics and graft function at biopsy					
Surveillance biopsy, n (%)	98 (84.5)	41 (56.2)	22 (68.8)	**<0.001**	0.281
Biopsy time after KT, months, median [IQR]	13.8 [12-17]	23.9 [13-83]	14.3 [12-37]	**<0.001**	**0.032**
HLA-DSA, n (%)	11 (9.6)	63 (86.3)*	0 (0)	**<0.001**	**<0.001**
Serum creatinine, mg/dl, mean ± SD	1.5 ± 0.6	1.9 ± 0.9	1.9 ± 1.0	**<0.001**	0.696
Estimated GFR, ml/min, mean ± SD	55.7 ± 22.8	44.1 ± 21.4	42.4 ± 23.4	**<0.001**	0.710
Urine protein/creatinine ratio, mg/g, median [IQR]	135.0 [90-244]	308.3 [158-1003]	458.1 [104-1023]	**<0.001**	0.838
Preceding CMV infection or disease, n (%)	33 (28.4)	19 (26.4)	10 (31.3)	0.875	0.610
Preceding BKV infection or disease, n (%)	12 (10.4)	3 (4.2)	2 (6.5)	0.285	0.621
Immunosuppressive treatment at biopsy					
Prednisone, n (%)	112 (96.6)	58 (79.5)	30 (93.8)	**<0.001**	0.086
Calcineurin inhibitors, n (%)	113 (97.4)	63 (86.3)	30 (93.8)	**0.009**	0.337
Mycophenolic acid, n (%)	94 (81.0)	55 (75.3)	21 (65.6)	0.171	0.347
mTOR inhibitors, n (%)	16 (13.8)	20 (27.4)	11 (34.4)	**0.012**	0.493
Treatment after ABMRh diagnosis					
Corticosteroids, n (%)	n.a.	7 (9.6)	4 (12.5)	n.a.	0.732
Intravenous Ig, n (%)	n.a.	8 (11.1)	0 (0)	n.a.	0.056
Plasmapheresis, n (%)	n.a.	4 (5.5)	0 (0)	n.a.	0.311
Rituximab, n (%)	n.a.	5 (6.9)	0 (0)	n.a.	0.320
Anti-thymocyte globulin, n (%)	n.a.	1 (1.4)	2 (6.7)	n.a.	0.203
Clazakizumab, n (%)	n.a.	1 (1.4)	0 (0)	n.a.	1.000
Optimization of immunosuppression, n (%)	n.a.	35 (48.0)	7 (21.9)	n.a.	**0.017**
End of follow-up					
5-year mortality after biopsy, n (%)	10 (8.6)	8 (11.0)	5 (15.6)	0.133	0.400
5-year death-censored graft loss after biopsy, n (%)	6 (5.2)	22 (30.1)	5 (15.6)	**<0.001**	0.162
Time from biopsy to end of follow-up, months, median [IQR]	59.7 [44-80]	34.6 [19-72]	36.8 [20-55]	**<0.001**	0.679
Time from KT to end of follow-up, months, median [IQR]	76.5 [60.9 – 92.5]	82.3 [46.8 – 163.9]	64.4 [35.7 – 88.7]	**0.047**	0.051

**ABMR cases without evidence of circulating HLA-DSA had linear C4d staining in peritubular capillaries or medullary vasa recta according to Banff 2019 criteria.*

572 *ABMR: antibody-mediated rejection; ABMRh: antibody-mediated rejection histology: BKV: Polyomavirus*
573 *or BK virus; CMV: cytomegalovirus; D: donor; GFR: glomerular filtration rate; HLA: human leukocyte*
574 *antigen; HLA-DSA: HLA donor-specific antibodies; iMVI: isolated microvascular inflammation; IQR:*
575 *interquartile range; KT: kidney transplantation; R: recipient; SD: standard deviation.*

Table 2. Comparison of histological features between groups.

	Normal (n=116)	ABMR (n=73)	iMVI (n=32)	p-value 3 groups	p-value ABMR vs. iMVI
Percentage of glomerulosclerosis (n, %)	9.5 (12.7)	15.2 (16.3)	14.4 (18.1)	**0.025**	0.830
g, mean ± SD	.08 ± .27	1.33 ± .97	1.84 ± .77	**<0.000**	**0.009**
g ≥1, n (%)	9 (7.8)	55 (75.3)	30 (93.8)	**<0.001**	**0.031**
ptc, mean ± SD	.16 ± .36	1.03 ± .73	.94 ± .84	**<0.000**	0.484
ptc ≥1, n (%)	18 (15.5)	55 (75.3)	21 (65.6)	**<0.001**	0.347
g ≥2 with ptc 0-1, n (%)	0 (0)	12 (52.2)	8 (66.7)	**<0.001**	0.489
ptc ≥2 with g 0-1, n (%)	0 (0)	1 (4.4)	2 (16.7)	0.230	0.266
MVI score, mean ± SD	.23 ± .42	2.34 ± 1.36	2.78 ± 1.07	**<0.000**	0.260
MVI (g + ptc ≥2), n (%)	0 (0)	57 (78.1)	32 (100)	**<0.001**	**0.002**
C4d, mean ± SD	.05 ± .32	1.08 ± 1.20	.13 ± .34	**<0.001**	**<0.001**
C4d ≥2, n (%)	1 (0.9) #	28 (38.4)	0 (0)	**<0.001**	**<0.001**
cg, mean ± SD	0	.61 ± .74	.56 ± .76	**<0.001**	0.699
cg, n (%)	0 (0)	33 (45.2)	13 (40.6)	**<0.001**	0.673
v, mean ± SD	0	.05 ± .21	.13 ± .55	0.050	0.711
v ≥1, n (%)	0 (0)	3 (4.6)	2 (6.3)	**0.023**	1.000
i, mean ± SD	.04 ± .20	.15 ± .40	.13 ± .55	0.055	0.288
i ≥1, n (%)	5 (4.3)	10 (13.7)	2 (6.3)	0.056	0.335
t, mean ± SD	0	.14 ± .38	.13 ± .55	**<0.001**	0.380
t ≥1, n (%)	0 (0)	9 (12.3)	2 (6.3)	**<0.001**	0.497
Concomitant borderline/TCMR changes*, n (%)	0 (0)	5 (6.8)	2 (6.3)	**0.006**	0.638
ci, mean ± SD	.93 ± .59	1.33 ± .67	1.5 ± .76	**<0.001**	0.225
ci ≥1, n (%)	92 (80.7)	69 (94.5)	30 (93.8)	**0.011**	1.000
ct, mean ± SD	.92 ± .55	1.25 ± .66	1.5 ± .80	**<0.001**	0.117
ct ≥1, n (%)	93 (80.2)	67 (91.8)	30 (93.8)	0.063	1.000
cv, mean ± SD	.76 ± .82	1.06 ± .95	1.39 ± .84	**0.001**	0.097
cv ≥1, n (%)	57 (52.8)	41 (63.1)	25 (80.6)	**0.017**	0.102
ah, mean ± SD	.37 ± .61	.96 ± 1.09	.74 ± .93	**0.001**	0.383
ah ≥1, n (%)	35 (30.2)	35 (47.9)	13 (40.6)	**0.034**	0.667
mm, mean ± SD	.02 ± .13	.19 ± .49	.29 ± .53	**<0.001**	0.264
mm ≥1, n (%)	2 (1.7)	12 (16.4)	8 (25.0)	**<0.001**	0.286

* Defined according to Banff 2019 criteria. All cases with concomitant borderline/TCMR changes had glomerulitis ≥1.

ABO-incompatible kidney transplantation.

ABMR: antibody-mediated rejection; ah: arteriolar hialinosis; ci: interstitial fibrosis; cg: chronic glomerulopathy; ct: tubular atrophy; cv: transplant arteriopathy; g: glomerulitis; i: interstitial inflammation; iMVI: isolated microvascular inflammation; mm: mesangial matrix expansion; MVI: microvascular inflammation; ptc: peritubular capillaritis; SD: standard deviation; t: tubulitis; TCMR: T-cell mediated rejection; v: endarteritis.

Figure 1. Peripheral blood T cell distribution: comparison between ABMR, iMVI, and Normal groups.

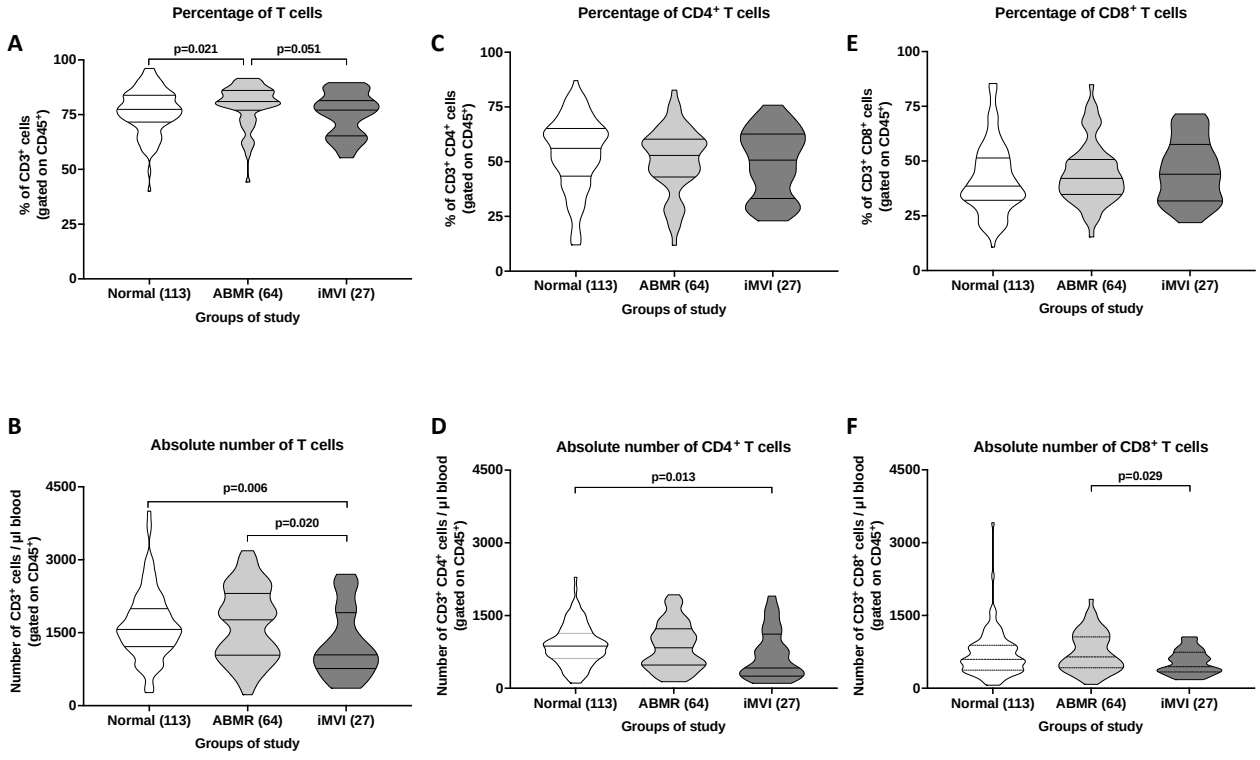

Figure 2. Peripheral blood NK cell distribution: comparison between ABMR, iMVI, and Normal groups.

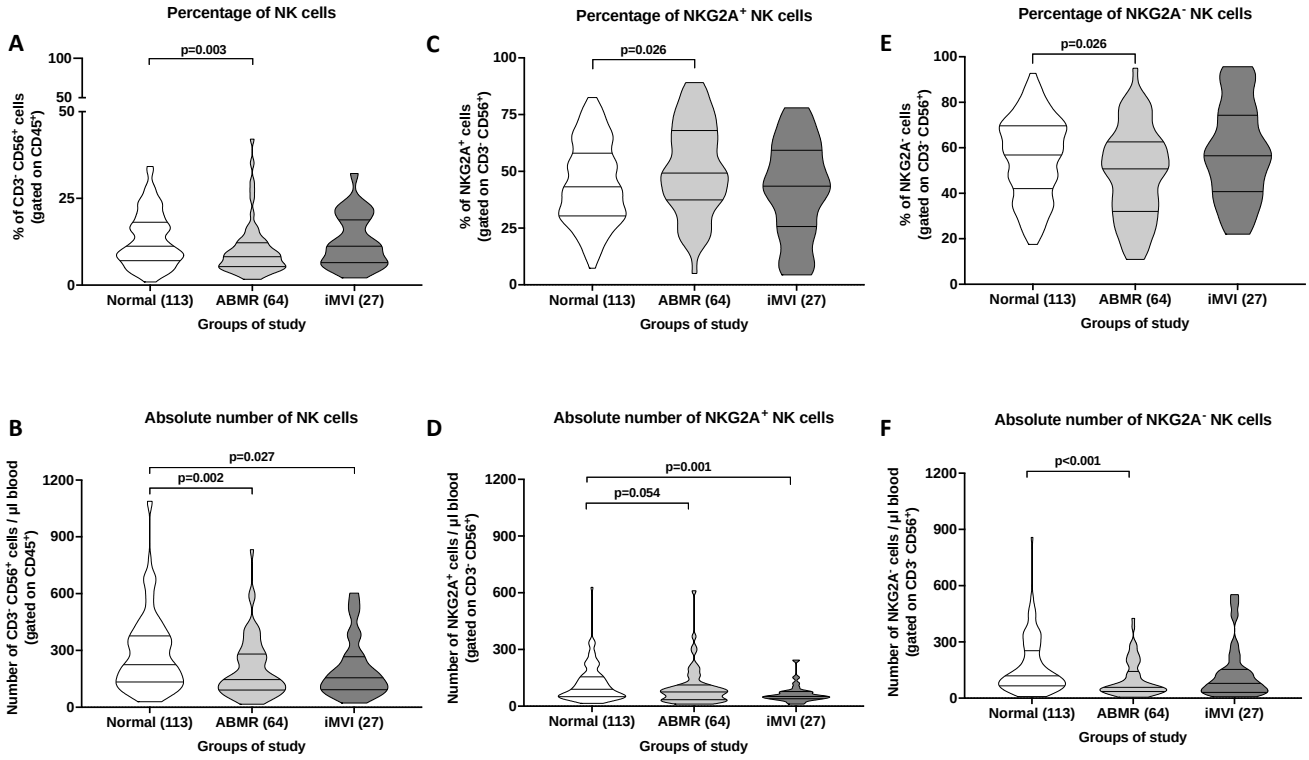

Figure 3. Immunohistochemistry assessment of leukocyte infiltration in the allograft: glomerular compartment.

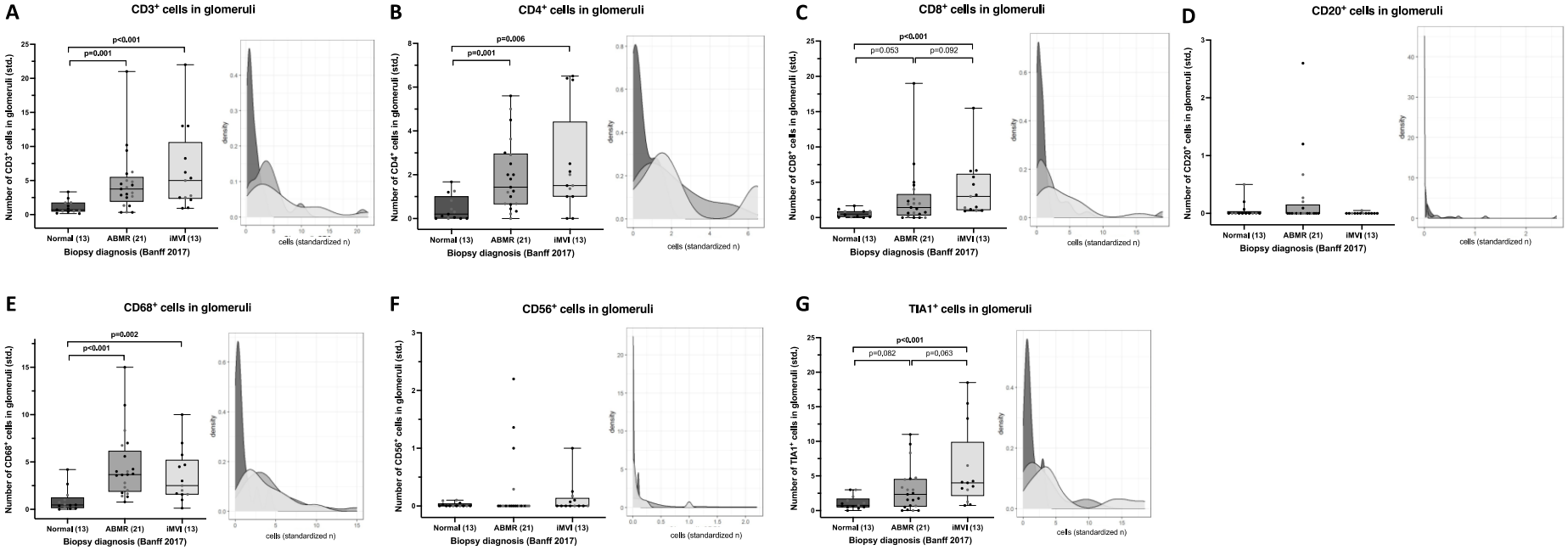

Figure 4. Immunohistochemistry assessment of leukocyte infiltration in the allograft: peritubular capillary compartment.

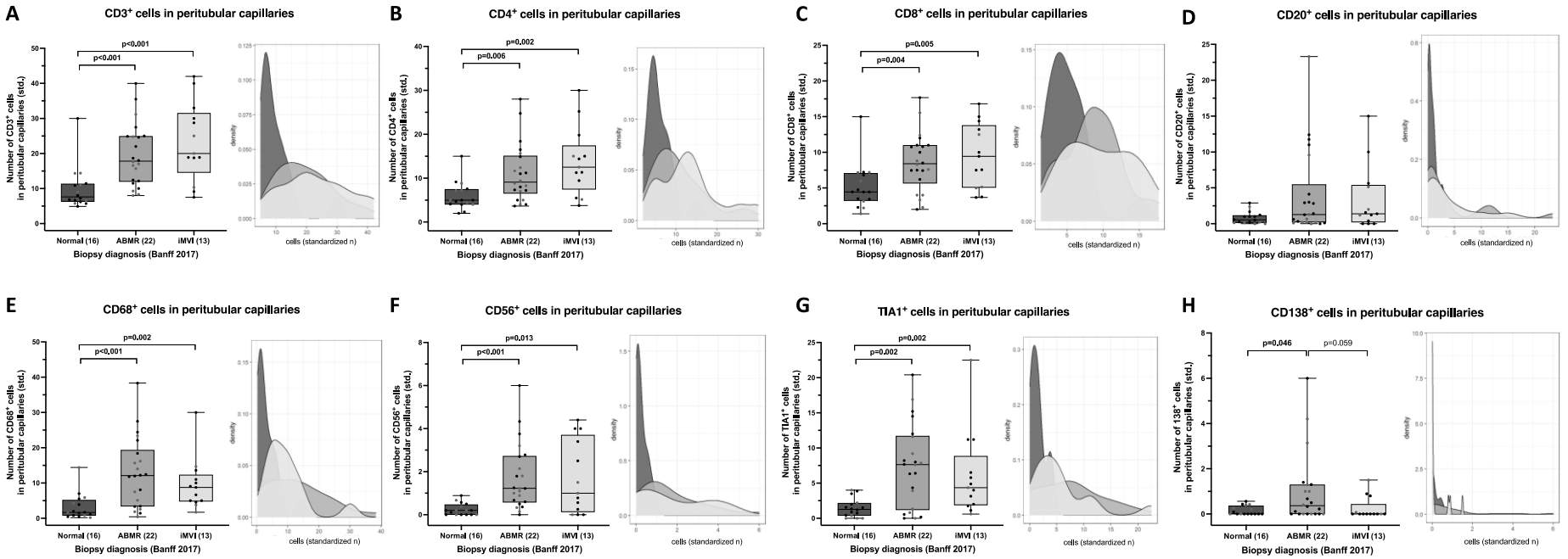

Figure 5. Immunohistochemistry assessment of leukocyte infiltration in the allograft: interstitial compartment (interstitial aggregates).

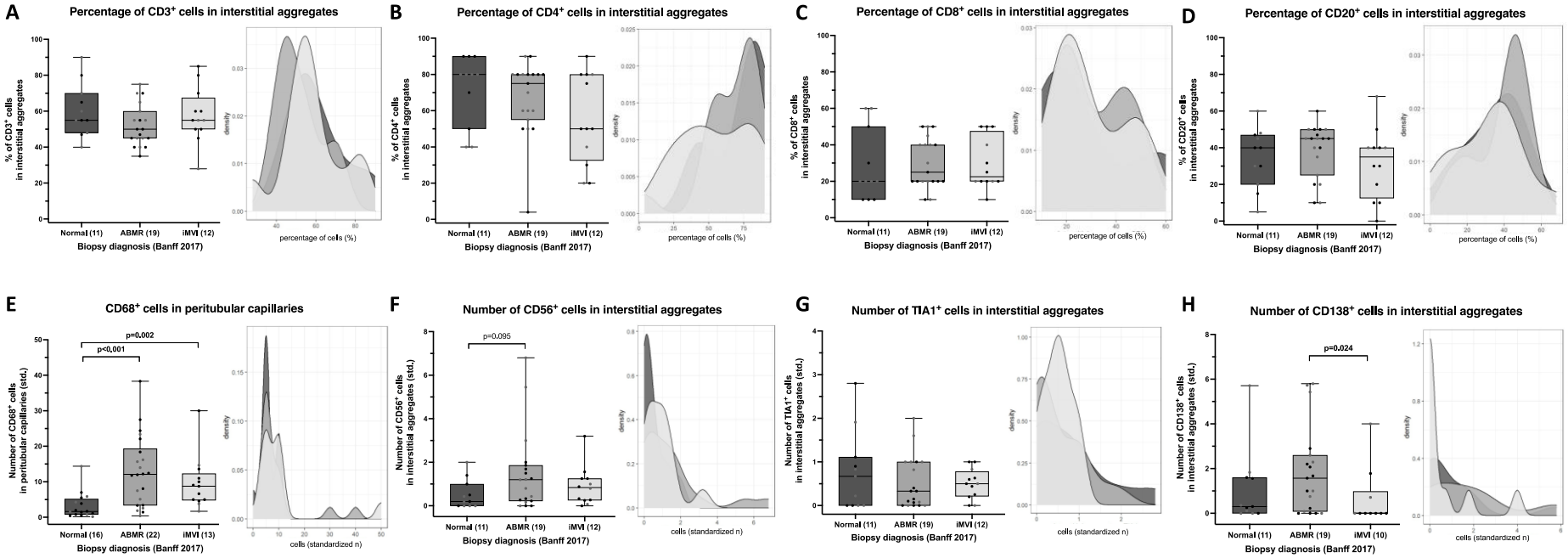

Figure 6. Association between leukocyte infiltration and the severity of histological features

A. Normal group

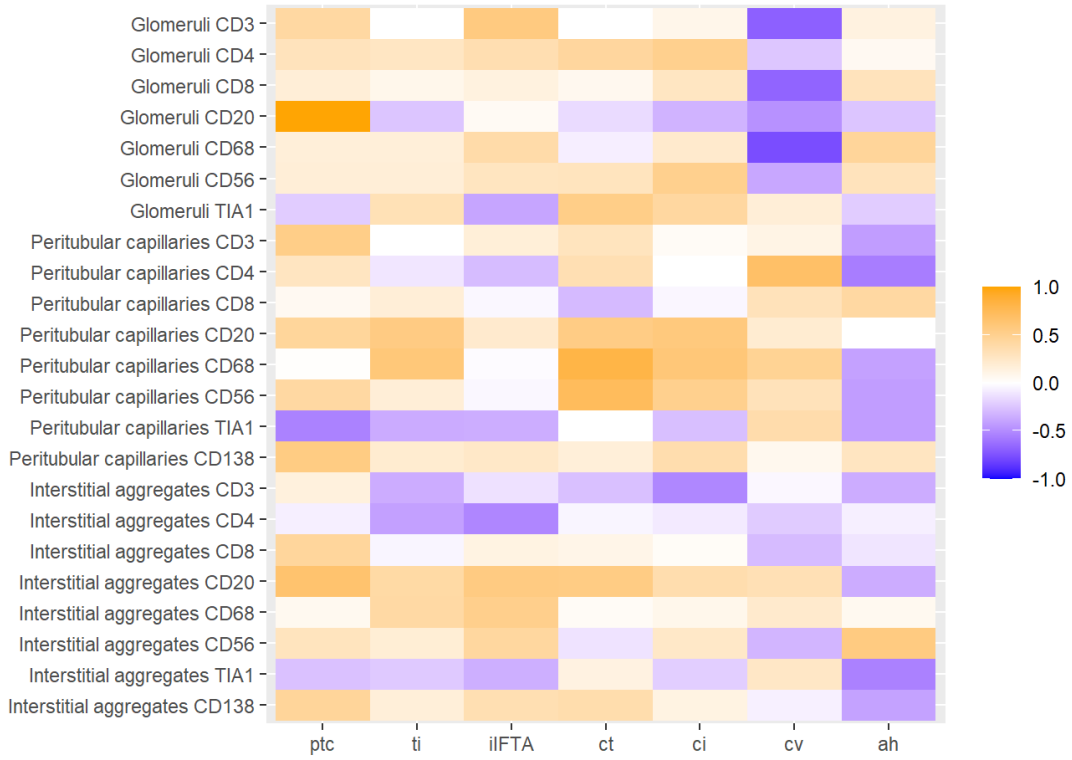

B. ABMR group

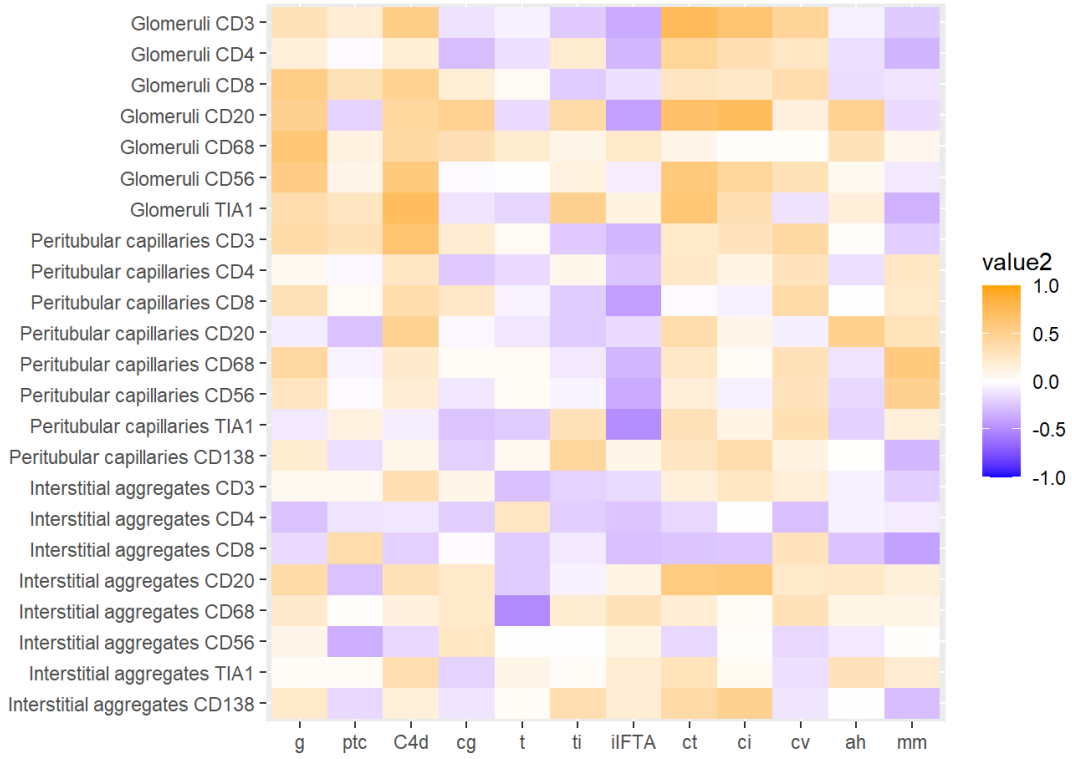

C. iMVI group

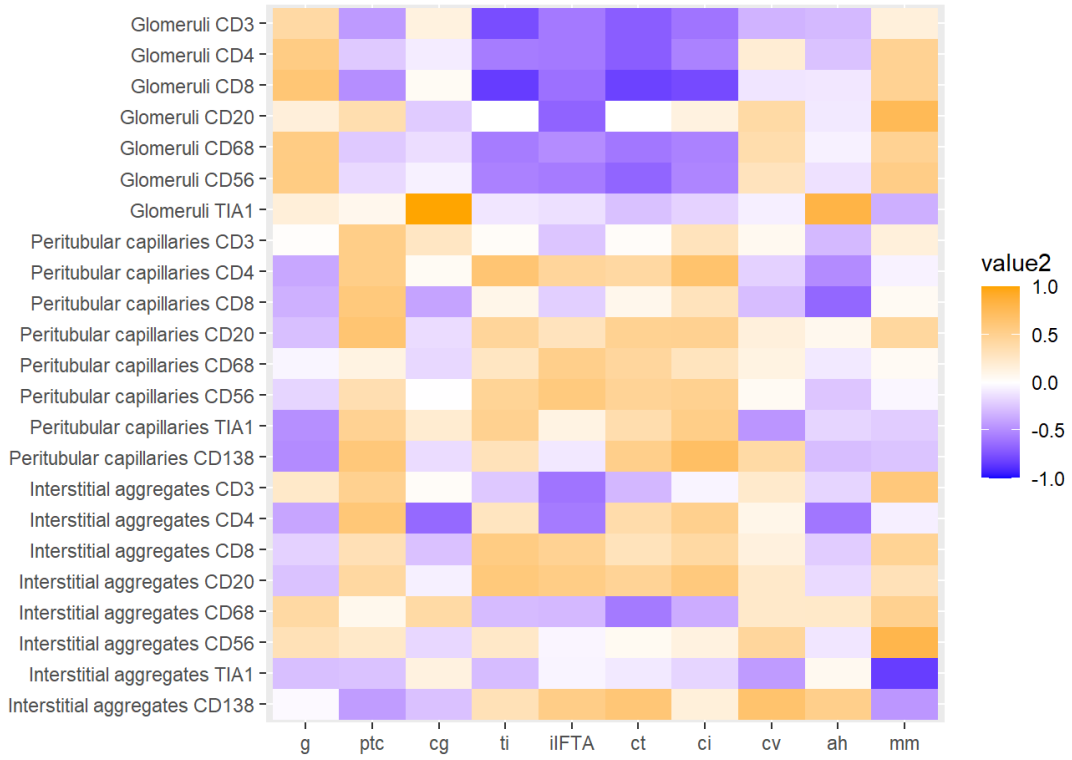
Glomeruli CD3
Glomeruli CD4
Glomeruli CD8
Glomeruli CD20
Glomeruli CD68
Glomeruli CD56
Glomeruli TIA1
Peritubular capillaries CD3
Peritubular capillaries CD4
Peritubular capillaries CD8
Peritubular capillaries CD20
Peritubular capillaries CD68
Peritubular capillaries CD56
Peritubular capillaries TIA1
Peritubular capillaries CD138
Interstitial aggregates CD3
Interstitial aggregates CD4
Interstitial aggregates CD8
Interstitial aggregates CD20
Interstitial aggregates CD68
Interstitial aggregates CD56
Interstitial aggregates TIA1
Interstitial aggregates CD138
g
ptc
cg
ti
iIFTA
ct
ci
cv
ah
mm
value2
1.0
0.5
0.0
-0.5
-1.0

Figure 7. Differential leukocyte infiltration in microvascular compartments from ABMR and iMVI lesions.

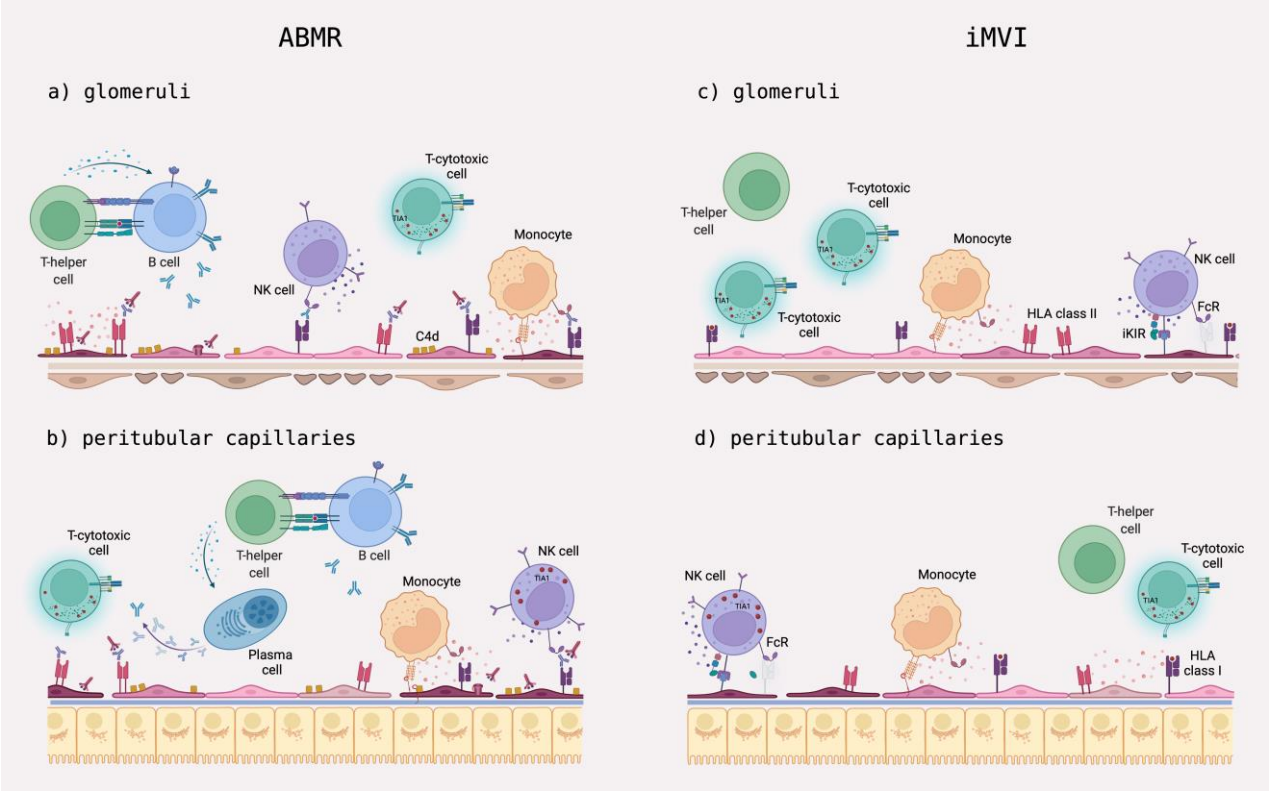

FIGURE LEGENDS

Figure 1. Peripheral blood T cell distribution: comparison between ABMR, iMVI and, Normal groups.

(A-F) Violin plots show the percentage and absolute numbers of T cells, $CD4^+$ T cells, and $CD8^+$ T cells in the peripheral blood. Plots show mean and standard error (SEM) for each study group. Mann-Whitney U-test was performed to compare peripheral blood T cell distribution among groups.

Figure 2. Peripheral blood NK cell distribution: comparison between ABMR, iMVI, and Normal groups.

(A-F) Violin plots show the percentage and absolute numbers of NK cells, $NKG2A^+$ cells, and $NKG2A^-$ cells in the peripheral blood. Plots show mean and standard error (SEM) for each study group. Mann-Whitney U-test was performed to compare peripheral blood T cell distribution among groups.

Figure 3. Immunohistochemistry assessment of leukocyte subset infiltration in the allograft: glomerular compartment.

(A-G) Box plots display standardized quantification of leukocyte subset infiltration in the glomeruli of kidney allografts with Normal histology, ABMR, and iMVI. Density plots are used to visualize the distribution of the quantification values. CD3, CD4, CD8, CD20, CD68, CD56, and TIA1 were used to quantify T cells, B cells, macrophages, NK cells, and cytotoxic infiltration, respectively. Cell count was standardized by dividing the number of cells by the total of glomeruli. Black dots represent FcγRIIIA 158-V carriers, and grey dots patients with 158-F/F-genotype. Plots show median and interquartile range (IQR) for each study group.

Figure 4. Immunohistochemistry assessment of leukocyte subset infiltration in the allograft: peritubular capillary compartment.

(A-H) Box plots display standardized quantification of leukocyte subset infiltration in the peritubular capillaries of kidney allografts with Normal histology, ABMR, and iMVI. Density plots are used to visualize the distribution of the quantification values. CD3, CD4, CD8, CD20, CD68, CD56, TIA1, and CD138 were used to quantify T cells, B cells, macrophages, NK cells, cytotoxic infiltration, and plasma cells, respectively. Cell count was standardized by dividing the number of cells by the length of the sample in mm. Black dots represent FcγRIIIA 158-V carriers and grey dots 158-F/F homozygotes. Plots show median and interquartile range (IQR) for each study group.

Figure 5. Immunohistochemistry assessment of leukocyte subset infiltration in the allograft: interstitial compartment (interstitial aggregates).

(A-H) Box plots display standardized quantification of leukocyte subset infiltration in the interstitial aggregates of kidney allografts with Normal histology, ABMR, and iMVI. Density plots are used to visualize the distribution of the quantification values. CD3, CD4, CD8, CD20, CD68, CD56, TIA1, and CD138 were used to quantify T cells, B cells, macrophages, NK cells, cytotoxic infiltration, and plasma cells, respectively. Cell count was standardized by dividing the number of cells by the length of the sample in mm. Black dots represent FcγRIIIA 158-V carriers and grey dots 158-F/F homozygotes. Plots show median and interquartile range (IQR) for each study group.

Figure 6. Association between leukocyte infiltration and the severity of histological features (N= 22 ABMR, 13 iMVI, 16 Normal cases).

Heatmap of Polyserial correlation between the topographical distribution of leukocyte subset infiltrates and the severity of histological lesions. A divergent gradient shows correlation intensity

where orange indicates a perfect association of ranks, white indicates no association, and blue indicates a perfect negative association of ranks. (**A**) Number of normal cases with complete data: 10/16 patients. Glomerulitis (g), C4d deposition, endarteritis (v), interstitial inflammation (i), tubulitis (t), and mesangial matrix expansion (mm) were not included because all subjects presented the same value. Therefore, the estimated variance is 0, and correlation cannot be estimated. Heatmap of Polyserial correlation in controls showed a positive correlation between $CD3^+$, CD4+, $CD20^+$ and $CD56^+$ and the peritubular capillaritis severity. Moreover, $CD3^+$, $CD68^+$, and $CD20^+$ in ptc correlated with the severity of IFTA. (**B**) Number of ABMR subjects with complete data: 17/22 patients. C4d deposition, endarteritis (v), and interstitial inflammation (i) were not included because all subjects presented the same value. Therefore, the estimated variance is 0, and correlation cannot be estimated. Heatmap of Polyserial correlation in ABMR showed a positive correlation between all glomerular leukocyte subtypes and the glomerulitis intensity. Contrariwise, any specific leukocyte subset infiltrates within ptc showed a strong positive correlation with the severity of ptc. (**C**) Number of iMVI subjects with complete data: 10/13 patients. Endarteritis (v), interstitial inflammation (i), and tubulitis (t) were not included because all subjects presented the same value. Therefore, the estimated variance is 0, and correlation cannot be estimated. Heatmap of Polyserial correlation in iMVI showed a strong correlation between $CD3^+$, $CD4^+$, $CD8^+$ and $CD56^+$ cells and the severity of glomerulitis and peritubular capillaritis. However, $CD68^+$ infiltrates were only associated with the severity of glomerulitis. Glomerular leukocyte infiltration in this group was inversely correlated with IFTA.

Figure 7. Differential leukocyte infiltration in microvascular compartments from ABMR and iMVI lesions.

This figure provides an overview of the major immunohistochemical findings when assessing the infiltrating immune cell composition in different microvascular compartments between ABMR and

iMVI. (**A**) Glomeruli of ABMR biopsies showed an immune cell landscape hallmarked by increased cytotoxic T cells and monocytes. (**B**) The inflammation in peritubular capillaries of ABMR biopsies predominantly consisted of circulating cytotoxic T cell and NK cells, monocytes, and plasma cells. (**C)** Glomerular infiltrating immune cell distribution in iMVI patients comprised increased cytotoxic T cells and monocyte inflammation. **D.** Leukocyte distribution in peritubular capillaries of iMVI biopsies was characterized by increased monocytes and cytotoxic T and NK cells. The absence of HLA-DSA and complement activation, together with scarce circulating plasma cells, suggest an antibody-independent immune activation in patients with iMVI.

This illustration was created with BioRender.